Storm phase dependence of ion outflow: Statistical signatures obtained by IMAGE/LENA

T. Kunori,[1] M. Nosé,[2] S. Taguchi,[3] K. Hosokawa,[3] M. R. Collier,[4] and T. E. Moore[4]

Received 2 March 2007; revised 30 April 2007; accepted 13 August 2007; published 28 September 2007.

[1] The low-energy neutral atom (LENA) imager on board the Imager for Magnetopause-to-Aurora Global Exploration (IMAGE) spacecraft can observe energetic neutral atoms (ENA) of 10 eV to a few keV generated by upflowing ions through charge exchange with the Earth's exosphere. Using IMAGE/LENA data, we statistically analyzed behaviors of the ion outflow in the main and recovery phases of the magnetic storms from June 2000 to December 2001. Results show that during the main phase, most of ENA emissions from the Earth's direction are accompanied by the solar wind dynamic pressure (P_{dy}) enhancements. For the recovery phase, there are no such tendencies. Instead, the ENA flux shows large values at the beginning of the recovery phase, and then decreases with the storm recovery. These results suggest that the dominant mechanism responsible for the ion outflow during the magnetic storms can be totally different between the two phases.
Citation: Kunori, T., M. Nosé, S. Taguchi, K. Hosokawa, M. R. Collier, and T. E. Moore (2007), Storm phase dependence of ion outflow: Statistical signatures obtained by IMAGE/LENA, *Geophys. Res. Lett.*, *34*, L18106, doi:10.1029/2007GL029877.

1. Introduction

[2] A number of numerical simulations have shown that the ions outflowing from the ionosphere can reach the nightside plasma sheet by calculating particle trajectory [e.g., *Chappell et al.*, 2000]. These results have suggested that ionospheric ions are one of the important sources of magnetospheric plasma. Thus it is important to reveal the properties of ion outflow from the ionosphere, which provides us the key to understand the dynamics of magnetosphere. It is well-known that the ion outflow has a dependence on geomagnetic activity [e.g., *Yau and André*, 1997]. The ion outflow rates are increased with the Kp index for both H^+ and O^+. In particular, the variations of the O^+ flux are more drastic in comparison with those of H^+. It was also reported that ion outflow is dependent on some solar wind parameters [e.g., *Cully et al.*, 2003], such as solar wind dynamic pressure (P_{dy}) and variations of IMF.

[3] The purpose of this study is to identify statistical different signatures of the ion outflow in the main and recovery phases of the magnetic storms. Although there may be different physical mechanisms between them, no studies have shown the storm phase dependence of the ion outflow. We tried to reveal the difference by using data obtained by the low-energy neutral atom (LENA) imager on board the Imager for Magnetopause-to-Aurora Global Exploration (IMAGE) spacecraft. A fraction of ions outflowing from the ionosphere and traveling along the magnetic field lines is converted into ENAs via the charge exchange with the Earth's exosphere. The generated ENAs keep almost the same energy and momentum as those before the charge exchange and if they have a speed that exceeds the gravitational escape speed (~10 km/sec), they can travel straight to the IMAGE spacecraft because they are no longer trapped by the magnetic field. Thus the LENA imager, which can observe ENA in low energy (10 eV to a few keV), enables us to remotely estimate the global variation of ion outflow in a short timescale although it is more difficult for in-situ measurements.

2. Observations

2.1. IMAGE/LENA

[4] The IMAGE spacecraft is a polar-orbiting satellite with a perigee of 1000 km altitude and an apogee of approximately 8.2 R_E [*Burch*, 2000]. The LENA imager on board the IMAGE spacecraft can observe the energetic neutral atom (ENA) in the energy range of 10 eV to a few keV [*Moore et al.*, 2000; *Collier et al.*, 2001]. In the present study we used the data combining the H and O peaks in the time of flight spectrum. The LENA imager field-of-view sweeps out 360° in azimuthal direction over a spin period (about 2 minutes) with a polar field-of-view of about ±45°. One complete 2-D image covers an area of 90° (polar) × 360° (azimuth) with 12 × 45 angular bins.

[5] The period of data analyzed here is from June 2000 to December 2001, excluding 2 months of December 2000 and January 2001 because the ENA emissions coming from the Earth direction in these two months were mostly the sun signal (ENA generated from solar wind ions) [*Collier et al.*, 2001]. Instrumental effects of the LENA imager during this 1.6-year period (e.g., voltage change of the micro channel plates and long-term degradation) are corrected. Since LENA count rate is expected to depend on the satellite altitude, we also corrected the LENA count rate by multiplying $\{(6.0 - 2.2)/(r - 2.2)\}^2$ [*Khan et al.*, 2003], where r is the geocentric distance of the IMAGE spacecraft in R_E.

2.2. Event Analysis

[6] We selected three consecutive satellite's orbits during a superstorm on 30–31 March 2001. Figure 1a shows the LENA count rate data summed over Earth-centered azimuthal range of −28° to +4° and polar range of −45°

[1]Department of Geophysics, Graduate School of Science, Kyoto University, Kyoto, Japan.
[2]Data Analysis Center for Geomagnetism and Space Magnetism, Graduate School of Science, Kyoto University, Kyoto, Japan.
[3]Department of Information and Communication Engineering, University of Electro-Communications, Tokyo, Japan.
[4]Laboratory for Extraterrestrial Physics, NASA Goddard Space Flight Center, Greenbelt, Maryland, USA.

Copyright 2007 by the American Geophysical Union.
0094-8276/07/2007GL029877

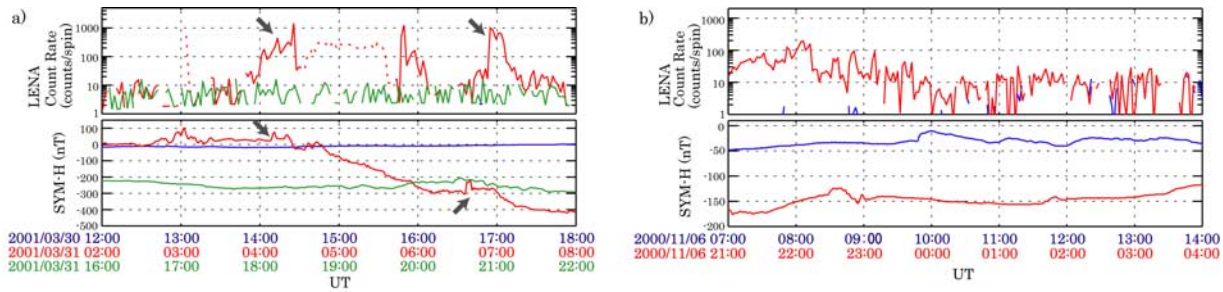

Figure 1. (a) LENA count rate summed over the Earth-centered azimuth of −28° to +4° on 30–31 March 2001 in three consecutive orbits and the SYM-H index. (b) LENA count rate summed over Earth-centered azimuth of −28° to +28° and the SYM-H index on 6–7 November in two consecutive orbits.

to +45° near apogees to see outflow flux as well as the SYM-H index during this interval. Different colors means different orbits; blue is the interval during quiet condition (from 1200 UT to 1800 UT on 30 March 2001), red is before the superstorm and during a storm main phase (from 0200 UT to 0800 UT on 31 March 2001), and green is during the recovery phase (from 1600 UT to 2200 UT on 31 March 2001). Throughout these intervals the LENA imager made an observation, and the LENA data are plotted as the IMAGE spacecraft was located in the almost same area if the x-coordinate is the same. Judging from 2-D images and result by *Moore et al.* [2003], we considered the data indicated by dotted lines contain not only outflow emissions but also sheath emissions [e.g., *Collier et al.*, 2005]. There are little count rates in LENA data in the first orbit, while in the second orbit LENA data showed an increase of background with ~10 counts/spin and some remarkable enhancements up to 100–1000 counts/spin. Since some of these enhancements of the LENA count rate were accompanied by sudden increases of the SYM-H index just after 0400 UT and around 0700 UT on 31 March 2001 as indicated by gray arrows, we considered the interplanetary shock as a possible trigger causing the sporadic enhancements of the LENA count rate. In the third orbit, we can also see the LENA emission comparable to the background count rate during the main phase but no clear sporadic enhancements.

[7] We selected another interval during a moderate magnetic storm on 6–7 November 2000 for further survey. Figure 1b shows LENA count rates summed over Earth-centered azimuthal range of −28° to +28° and polar range of −45° to +45° with correction of sun signal, and the SYM-H index for this interval in the same format as Figure 1a. The LENA imager was operating throughout this interval. While the LENA flux was mostly less than one-count level of the instrument in the first orbit (during a comparatively quiet interval, blue), the LENA count rate in the second orbit (during the recovery phase, red) showed gradual increase during 2100–2200 UT and reached the maximum just after the SYM-H index showed the minimum value. Then LENA count rate decreased gradually with the storm recovery and maintained around 10 counts/spin after 0000 UT on 7 November.

[8] From these event analyses we found that some sporadic LENA enhancements were accompanied by the sudden increase in the SYM-H index (possibly corresponding to interplanetary shocks) mainly during the main phase; and LENA count rate showed the highest values around the time of the minimum of the SYM-H index, followed by a gradual decrease during the storm recovery.

2.3. Statistical Analysis

[9] In order to examine the different signatures of LENA emission between storm main phase and recovery phase in more detail, we performed a statistical study. We used the LENA data when the IMAGE spacecraft was located at geomagnetic latitude of ≥60° and geocentric altitude of 4.5 R_E to 8.5 R_E. This is because we intended to limit satellite position to high latitudes near apogee, where ENAs generating from the outflowing ions can be viewed overall. The data taken when the spacecraft was outside the magnetosphere are not included, because the effects of magnetosheath emission lead to difficulties in distinguishing between magnetosheath and non-magnetosheath ENA. We summed the LENA count rate over the angular sectors which cover a region of geocentric altitude below 2 R_E, thus the effect of ring current ions near the equatorial plane around L = 4 can be neglected.

[10] We chose 29 magnetic storms with the minimum value of the SYM-H index below −70 nT in the aforementioned period, and examined the LENA data during the storm main and recovery phases of these storms. In order to define the storm main and recovery phases, we used the running average of the SYM-H index with the time window of 60 minutes (SYM-H_{RA}). The storm main phase is defined as the period when the SYM-H_{RA} decreased from −20 nT to 90% of the minimum of SYM-H_{RA}. The recovery phase is the period when the SYM-H_{RA} increased from 90% of the SYM-H_{RA} minimum up to −40 nT.

[11] The relation between the SYM-H_{RA} and the LENA count rate for the main phase and the recovery phase are shown in Figures 2a and 2b. When the LENA count rate is 3 or more per spin, we plotted the count rate by a small circle as a function of the SYM-H_{RA} at 6 minutes before the LENA measurement, to account for the transit time of ENA from the ionosphere to the IMAGE spacecraft. The SYM-H_{RA} data shown here is averaged over 2 minutes corresponding to the LENA data. We calculated the average value and the median value of the LENA count rate in each bin bounded by vertical dotted lines, and plotted them with green diamonds and red triangles, respectively. The median values of LENA count rate as well as correlation coeffi-

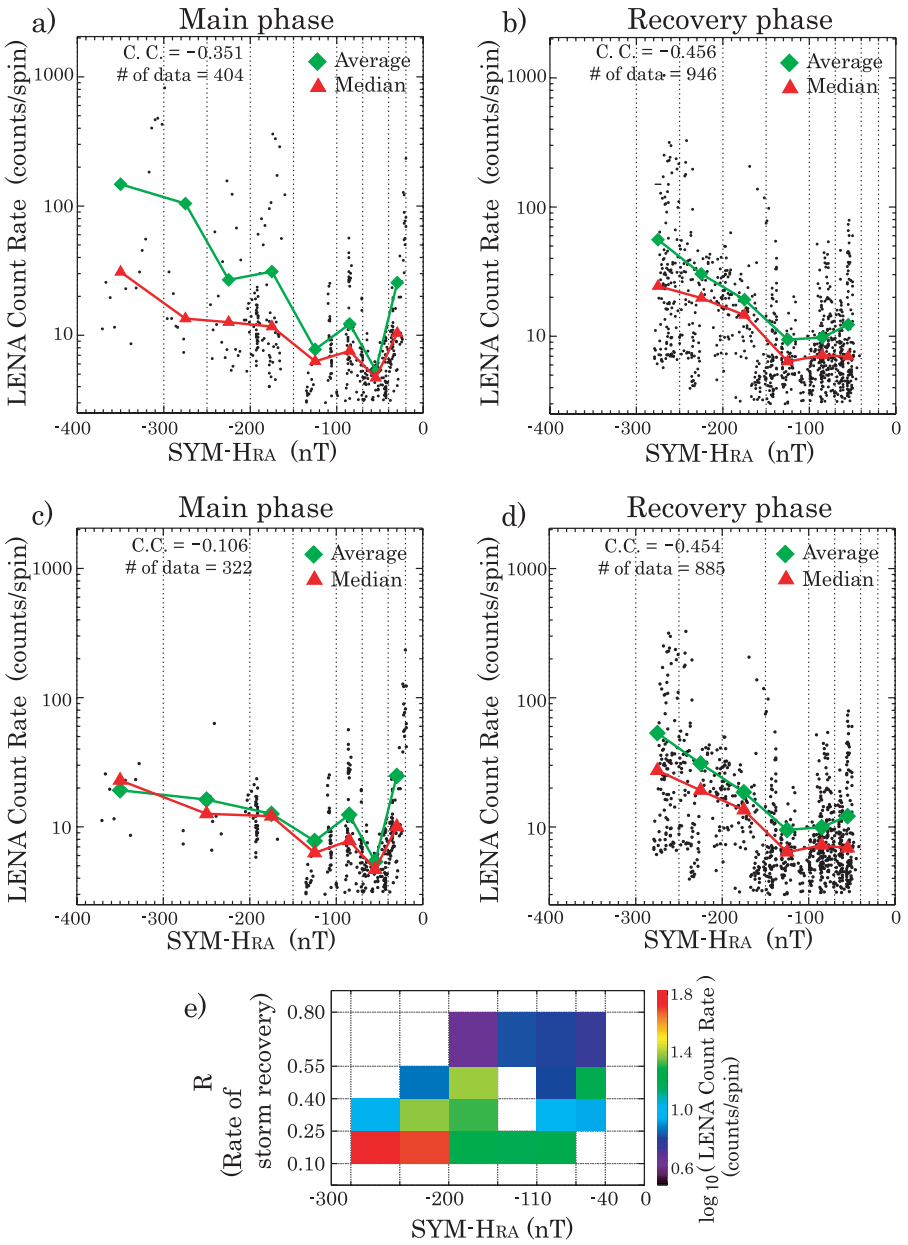

Figure 2. (a, b) Scatter plots of the LENA count rate from the Earth direction as a function of the SYM-H_{RA} during the storm main phase and during the storm recovery phase. (c, d) The same as Figures 2a and 2b except for the LENA count rate after excluding the count rate data accompanied by enhancements of P_{dy} or the SYM-H index. (e) The dependences of the LENA count rate from the Earth direction during the storm recovery phase on R and the magnitude of the SYM-H_{RA}.

cients are not much different between the main and recovery phases. However, the average values showed different signatures in terms of the dependence of the LENA count rate on the SYM-H_{RA}. The average values of LENA count rate during the recovery phase increased rather smoothly with decreases of the SYM-H_{RA} (Figure 2b), while those during the main phase showed overall increase with some bumps and dents (Figure 2a). The differences between average values and median values are larger in Figure 2a than Figure 2b, indicating more sporadic large count rates are included during the main phase. We think that these sporadic enhancements of the LENA count rate were mainly caused by the occurrence probability of interplanetary shocks. This is consistent with the result of Figure 1a.

[12] Next, we examined how frequently the increases of LENA count rates are accompanied by P_{dy} enhancements, which is observed by ACE/SWEPAM. Propagation time of solar wind from the ACE spacecraft to the magnetopause was considered. When the LENA count rate is larger than a given threshold, we examined if this large LENA count rate is preceded by the P_{dy} enhancements within 20 minutes. The P_{dy} enhancement was defined as the increase of 4 nPa within 128 seconds. Occurrence probability of the LENA count rate data preceded by P_{dy} enhancements for different thresholds is shown in Figure 3. In Figures 3a and 3b we

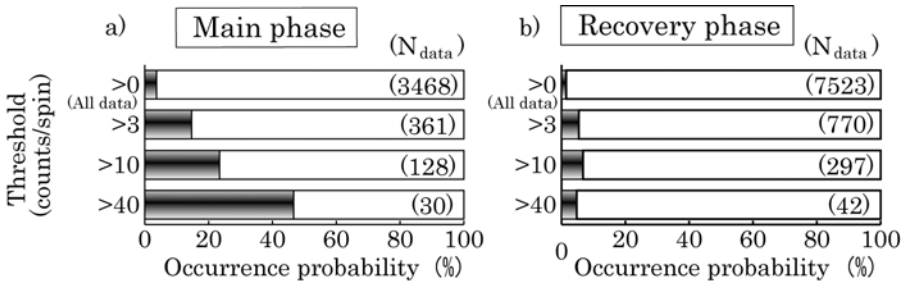

Figure 3. Occurrence probability of the LENA count rate data preceded by P_{dy} enhancements obtained by ACE/SWEPAM for different thresholds (a) during the main phase and (b) during the recovery phase. N_{data} means the number of all the count rate data over the threshold.

changed the threshold of LENA count rates as 0, 3, 10, 40 counts/spin (the threshold of 0 count/spin corresponds to consideration of all LENA data). The differences between two phases can be seen apparently. Though the probability of the enhancement of P_{dy} was increased with the rise of the threshold of the LENA count rate during the main phase, the similar feature was hardly seen during the recovery phase. Moreover, the probability of the enhancements of P_{dy} in the main phase are higher than those in the recovery phase in all thresholds of the LENA count rates.

[13] Instead of solar wind data, we used the SYM-H index and performed the similar analysis, because the enhancements of P_{dy} are usually accompanied by those of the SYM-H index. The definition of an enhancement of the SYM-H index is an increase of more than 10 nT within 2 minutes. From this analysis, we again found the clear difference between the main phase and the recovery phase, which is almost the same as the above analysis (not shown here).

[14] We excluded from Figures 2a and 2b the LENA count rate data accompanied by the enhancement of P_{dy} or the SYM-H index. The result is shown in Figures 2c and 2d in the same format as Figure 2a and 2b. In the main phase (Figure 2c), there are little large count rates, and the average and median values are around 10 counts/spin. This is consistent with the background LENA count rates (~10 counts/spin) shown in Figure 1a. In contrast, during the recovery phase, there are still much more ENA emissions with large count rates (Figure 2d), especially at the large negative SYM-H_{RA}.

[15] In the recovery phase (Figure 2d), we can see the scatter of the LENA count rate at the large negative SYM-H_{RA}. We suppose that this scatter may be due to the rate of the storm recovery (R) which is defined by $R = 1 - (\text{SYM-}H_{RA})/(\text{SYM-}H_{RA}\ \text{minimum})$. Figure 2e shows the dependence of the LENA count rate on both the magnitude of the SYM-H_{RA} and R. We can find that the average value of the LENA count rate tends to be higher at small R than at large R when the SYM-H_{RA} is the same. The LENA count rate shows the largest values when the SYM-H_{RA} is largely negative and R is small. Thus we suggest that the scatter of the LENA count rate at large negative SYM-H_{RA} in Figure 2d represent different rates of the storm recovery in magnetic storms. In the 6–7 November 2000 event (Figure 1b), the maximum value of LENA count rate is observed around the beginning of the storm recovery. We think that this maximum LENA count rates includes both the effects of the largely negative SYM-H index and the small rate of the storm recovery. These results imply a particular mechanism responsible for ion outflows during the recovery phase. For example, ion outflows during the recovery phase may be closely related to the fast storm recovery, which occurs at the beginning of the storm recovery.

3. Discussion

3.1. Main Phase

[16] It is found that during the storm main phase, most of the large ENA emissions from the Earth direction are accompanied by P_{dy} enhancements (Figure 3a). The relation between the interplanetary shock and the ion outflow has been discussed by previous researches. The flux of ion outflows is increased with the increase in P_{dy} [e.g., *Cully et al.*, 2003]. *Moore et al.* [1999, 2001] and *Khan et al.* [2003] reported that the ion outflow flux was enhanced promptly (~2min) when the CME shock passed the magnetosphere. *Nosé et al.* [2006] reported that the ENA emissions are enhanced at substorm onset, some of which are accompanied by P_{dy} enhancements. Thus the large ENA emissions during the main phase may be explained by the ion outflows which were generated by shock-triggered substorms.

[17] There is another possible mechanism related to the dayside aurora which can be observed when an interplanetary shock arrived at the magnetosphere [e.g., *Liou et al.*, 2002]. The close relation between ion outflows and the auroral region is well-known, so the ion outflows may be generated over the dayside auroral region accompanied by the interplanetary shock.

3.2. Recovery Phase

[18] We found the following two features of ion outflows during recovery phase: the occurrence probability of large ENA emissions accompanied by the sudden increase of P_{dy} was much lower than during the main phase (Figure 3b); and ENA emissions showed the highest value at the beginning of the storm recovery (Figures 1b and 2e). From the former result, we supposed that the signature of ion outflows during the recovery phase is different from that of the main phase. The latter result indicates that at the beginning of storm recovery there are particular mechanisms which increase the density or the speed of ion outflow.

[19] If the density increase of ion ouflow is responsible for the high ENA emission, it may be caused by a larger scale height in the topside ionosphere. It is noted that the ions or electrons in the topside ionosphere can be heated by the particle precipitation, resulting in the increase of the scale height. The precipitating ions with energy less than a few keV can heat topside ionospheric ions effectively [e.g., *Ishimoto et al.*, 1992]. *Walt and Voss* [2001] reported that precipitating ion flux obtained by Polar/SEPS were much higher near the minimum Dst than during a quiet interval and the late recovery phase. *Jordanova et al.* [2001] suggested that pitch angle scattering of ring current ions in the energy range of 1–50 keV into the loss cone can be enhanced during a magnetic storm by electromagnetic ion cyclotron (EMIC) waves.

[20] Soft electron precipitation can heat ionospheric electrons, which is frequently accompanied by initial ion upflows in the topside ionosphere. During the recovery phase, the electrons near the expanding plasmapause may be heated by Coulomb collisions with ring current ions and precipitate along the magnetic field into the ionosphere at F region heights. These heated electrons are considered to contribute to the stable aurora red arc [*Kozyra et al.*, 1987]. Since the soft electron precipitation is considered to occur during the early recovery phase, this mechanism may explain the observed feature during the recovery phase.

[21] On the other hand, if the increase of the speed of ion outflows is the case, ion outflows should be further accelerated by some mechanisms. Wave-particle interaction and parallel electric field are famous mechanisms closely related to the acceleration of ions. In the former mechanism, ions interact with the broad-band low-frequency waves [e.g., *André and Yau*, 1997]. The latter mechanism can be seen in the double layer above the auroral region or in association with the kinetic Alfvén wave.

[22] We cannot distinguish between the changes of the density and the speed of ion outflows since the LENA imager does not have the energy resolution. Further studies using simultaneous observation by the LENA imager and in-situ instruments at low altitude are required to solve this issue.

4. Conclusions

[23] We investigated the signatures of the ENA emission in low energy from the Earth direction during magnetic storms and obtained the following conclusions. (1) The P_{dy} enhancements predominantly control ion outflows during the storm main phase, but do not during the recovery phase. (2) During the early recovery phase, there can be a particular mechanism responsible for ion outflows. A possible mechanism is soft electron precipitation from the plasmasphere via the Coulomb collision with the ring current ions. (3) The dominant mechanism responsible for the ion outflow during the magnetic storms can be totally different between the two phases.

[24] **Acknowledgments.** The SYM-H index was provided by T. Iyemori at WDC for Geomagnetism, Kyoto. We also thank D. McComas, the ACE/SWEPAM instrument team, and the ACE Science Center for providing the ACE data. This work was partially supported by the Sumitomo Foundation (grant 030677) and the MEXT, Grant-in-Aid for Young Scientists (B) (grant 17740327) and Category (C) (grant 18540443).

References

André, M., and A. W. Yau (1997), Theories and observations of ion energization and outflow in the high latitude magnetosphere, *Space Sci. Rev.*, *80*, 27–48.

Burch, J. L. (2000), IMAGE mission overview, *Space Sci. Rev.*, *91*, 1–14.

Chappell, C. R., et al. (2000), The adequacy of the ionospheric source in supplying magnetospheric plasma, *J. Atmos. Sol. Terr. Phys.*, *62*, 421–436.

Collier, M. R., et al. (2001), Observations of neutral atoms from the solar wind, *J. Geophys. Res.*, *106*, 24,893–24,906.

Collier, M. R., T. E. Moore, M.-C. Fok, B. Pilkerton, S. Boardsen, and H. Khan (2005), Low-energy neutral atom signatures of magnetopause motion in response to southward B_z, *J. Geophys. Res.*, *110*, A02102, doi:10.1029/2004JA010626.

Cully, C. M., E. F. Donovan, A. W. Yau, and G. G. Arkos (2003), Akebono/Suprathermal Mass Spectrometer observations of low-energy ion outflow: Dependence on magnetic activity and solar wind conditions, *J. Geophys. Res.*, *108*(A2), 1093, doi:10.1029/2001JA009200.

Ishimoto, M. I., G. J. Romick, and C.-I. Meng (1992), Energy distribution of energetic O^+ precipitation into the atmosphere, *J. Geophys. Res.*, *97*, 8619–8629.

Jordanova, V. K., C. J. Farrugia, R. M. Thorne, G. V. Khazanov, G. D. Reeves, and M. F. Thomsen (2001), Modeling ring current proton precipitation by electromagnetic ion cyclotron waves during the May 14–16, 1997, storm, *J. Geophys. Res.*, *106*, 7–22.

Khan, H., M. R. Collier, and T. E. Moore (2003), Case study of solar wind pressure variations and neutral atom emissions observed by IMAGE/LENA, *J. Geophys. Res.*, *108*(A12), 1422, doi:10.1029/2003JA009977.

Kozyra, J. U., E. G. Shelley, R. H. Comfort, L. H. Brace, and T. E. Cravens (1987), The role of ring current O^+ in the formation of stable auroral red arcs, *J. Geophys. Res.*, *92*, 7487–7502.

Liou, K., C.-C. Wu, R. P. Lepping, P. T. Newell, and C.-I. Meng (2002), Midday sub-auroral patches (MSPs) associated with interplanetary shocks, *Geophys. Res. Lett.*, *29*(16), 1771, doi:10.1029/2001GL014182.

Moore, T. E., W. K. Peterson, C. T. Russell, M. O. Chandler, M. R. Collier, H. L. Collin, P. D. Craven, R. Fitzenreiter, B. L. Giles, and C. J. Pollock (1999), Ionospheric mass ejection in response to a CME, *Geophys. Res. Lett.*, *26*, 2339–2342.

Moore, T. E., et al. (2000), The low energy neutral atom imager for IMAGE, *Space Sci. Rev.*, *91*, 155–195.

Moore, T. E., et al. (2001), Low energy neutral atoms in the magnetosphere, *Geophys. Res. Lett.*, *28*, 1143–1146.

Moore, T. E., et al. (2003), Heliosphere-geosphere interactions using low energy neutral atom imaging, *Space Sci. Rev.*, *109*, 351–371.

Nosé, M. et al. (2006), Simultaneous observations of ions of ionospheric origin over the ionosphere and in the plasma sheet at storm-time substorms, in *Proceedings of the Eighth International Conference on Substorms*, edited by M. Syrjäsuo and E. Donovan, pp. 203–208, Univ. of Calgary, Alberta.

Walt, M., and H. D. Voss (2001), Losses of ring current ions by strong pitch angle scattering, *Geophys. Res. Lett.*, *28*, 3839–3842.

Yau, A. W., and M. André (1997), Sources of ion outflow, *Space Sci. Rev.*, *80*, 1–25.

M. R. Collier and T. E. Moore, Laboratory for Extraterrestrial Physics, NASA Goddard Space Flight Center, Greenbelt, MD 20771, USA.

K. Hosokawa and S. Taguchi, Department of Information and Communication Engineering, University of Electro-Communications, Chofugaoka 1-5-1, Tokyo 182-8585, Japan.

T. Kunori, Department of Geophysics, Graduate School of Science, Kyoto University, Oiwake-cho, Kitashirakawa, Sakyo-ku, Kyoto 606-8502, Japan. (kunori@kugi.kyoto-u.ac.jp)

M. Nosé, Data Analysis Center for Geomagnetism and Space Magnetism, Graduate School of Science, Kyoto University, Oiwake-cho, Kitashirakawa, Sakyo-ku, Kyoto 606-8502, Japan.